VIII International Conference on Fracture Mechanics of Concrete and Concrete Structures
FraMCoS-8
J.G.M. Van Mier, G. Ruiz, C. Andrade, R.C. Yu and X.X. Zhang (Eds)

SOME ISSUES ON PREDICTION OF MASSIVE STRUCTURES CRACKING AT EARLY AGE

A. HILAIRE*, F.BENBOUDJEMA*, A.DARQUENNES*, Y.BERTHAUD† AND G.NAHAS‡

*LMT/ENS Cachan
61 Avenue du Président Wilson, 94230 Cachan, FRANCE.
e-mail: hilaire,benboudjema,darquennes@lmt.ens-cachan

†Université Paris 6
4 place Jussieu, Paris, FRANCE
e-mail: berthaud@lmt.ens-cachan

‡IRSN
Fontenay-aux-Roses, FRANCE
e-mail: georges.nahas@irsn.fr

Key words: Early age, creep, sustainability, massive structure

Abstract. At early age, massive structures are prone to thermal cracking and may be damaged by the restraint of the thermal strain. Thermal and mechanical analysis have to be relevant to perform reliable numerical simulations. However, some uncertainties still remains: for instance, the values of the creep's compliance differed in the literature. Creep strains modeling is performed by a rheological model, the evolution of hydration, the long term viscoelasticity and the asymmetry of the behavior between tension and compression are taken into account. The influence of this dissymmetry is assessed throughout the casting of a massive wall on a raft foundation. The results show that the final damage field is highly dependent on the value of this dissymetry.

1 INTRODUCTION

The extension of the lifespan of nuclear plants (beyond 40 years) is a persistent question of France energy policy. The serviceability of the containment building beyond the expected operating life is a controversial subject. This structure is the last barrier of security and has to be completely sealed. A relevant prediction of the cracking state is needed to evaluate the impact of the ageing on the containment.
Cracking may occur at the early age and induces a reduction of the durability of the structure. For instance, during the casting process, tensile stresses are generated at the construction joint because of the restraint caused by the previous lift. Chemical and environmental phenomenons drive the development of the volume changes in concrete: the exothermic cement hydration reactions generate thermal strains and autogenous shrinkage happens simultaneously.
Tensile creep has to be considered to have a correct estimation of the stress state in concrete [2]. However, there is still a lot of uncertainties on the compliance of concrete's creep. According to some experimental results, the creep behavior seems to be different in tension and compression [8] [12] [11] [7] [1] [14] [6] [15](Fig. 1). This distinction is usually not taken into account, to the author's knowledge. The objective of this study is to underline the influence of this dissymetry on the early-age cracking of massive structures. The sealing of the damaged ar-

eas may be partially restored thanks to the prestressing operation and the relaxation of concrete. However, they remains weakness areas in case of an accident.

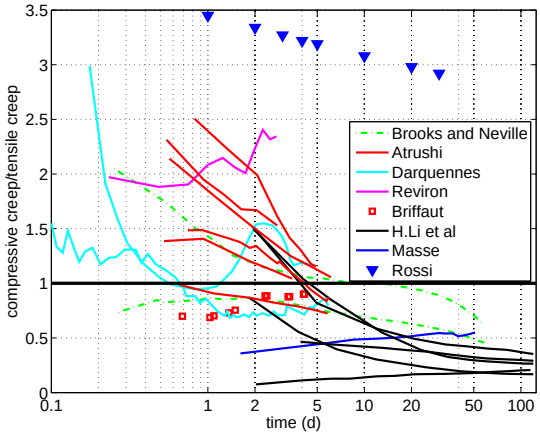

Figure 1: Compressive basic creep divided by tensile basic creep

2 MECHANICAL AND CHEMO-THERMAL MODELING

For each part of the modeling, the governing equations are described and the choice of the parameters is done by comparison with experimental data. These date are obtained from the concrete used for the casting of two reinforced concrete wall [2].

2.1 Chemo-thermal modeling

It is well known that the cement hydration is exothermic and thermo-activated. The kinetics of the hydration reaction is described thanks to an Arrhenius law (Eq. 1) in which ξ is the hydration degree, E_a is the activation energy, R is the constant of perfect gaz, T is the temperature and $\tilde{A}(\xi)$ is the normalized affinity [16].

$$\dot{\xi} = \tilde{A}(\xi) exp(-\frac{E_a}{RT}) \tag{1}$$

The evolution of the temperature is governed by the thermal diffusion equation (Eq. 2) where L is the latent heat of hydration, k_{th} is the thermal conductivity and C is the heat capacity.

$$C\dot{T} = \nabla(k_{th}\nabla T) + L\dot{\xi} \tag{2}$$

The thermal strain ϵ_{th} is proportional to the temperature variation thanks to the thermal expansion coefficient α_{th} (Eq. 3).

$$\dot{\epsilon_{th}} = \alpha_{th}\dot{T}\mathbb{1} \tag{3}$$

The values of the different parameters are summarized in the table 2.1 and the normalized affinity is plotted on the figure 2.

Table 1: Thermal parameters

$k_{th}(W.m^{-1}.K^{-1})$	3.05
$C(J.m^{-3}.K^{-1})$	2400
$L(J.m^{-3})$	154.7 10^6
$E_a/R(K^{-1})$	4400
$\alpha_{th}(K^{-1})$	12 10^{-6}

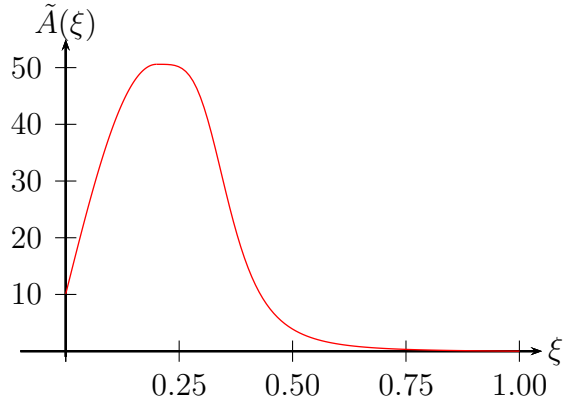

Figure 2: Evolution of the normalized affinity $\tilde{A}(\xi)$ versus the hydration degree ξ

2.2 Modeling of basic creep

Rheological model Several explanations are proposed to explain the difference between tensile and compressive creep: microcracking [15], debonding at the paste-aggregate interface [3], the elastic modulus is different in tension and in compression [7]. A one-dimensional rheological model with only 4 parameters is proposed to predict creep strains (Fig. 3(a)). The system of equations (Eq. 4) presents its governing equations and creep strains under a loading of $\mid \sigma \mid = 1MPa$ are plotted on the figure 3(b) where k_{bc} is kept constant and $\eta = k_{bc}\tau$. Therefore, only 4 parameters (for 1 Kelvin-Voigt unit

and 1 dashpot unit) need to be identified to estimate creep strains in concrete, from early-age to long term, including the partial recovery and the asymmetric behavior tension/compression.

$$\dot{\epsilon_{bc}} = \dot{\epsilon_{kv}} + \dot{\epsilon_{am}} \tag{4a}$$

$$\dot{\epsilon_{kv}} = \frac{\dot{\sigma} - \dot{\sigma_{ea}}}{k_{bc}(\xi)} \tag{4b}$$

$$\dot{\epsilon_{kv}} = \frac{\sigma_{ea}}{\eta} \tag{4c}$$

$$\dot{\epsilon_{am}} = \alpha \frac{< \sigma >_+}{\eta_a(t)} + \frac{< \sigma >_-}{\eta_a(t)} \tag{4d}$$

This system of equations leads to a second-order differential equation (Eq. 5).

$$\frac{\dot{\sigma}}{k_{bc}} = \tau \ddot{\epsilon_{kv}} + (1 + \frac{\dot{k_{bc}}}{k_{bc}}\tau)\dot{\epsilon_{kv}} \tag{5}$$

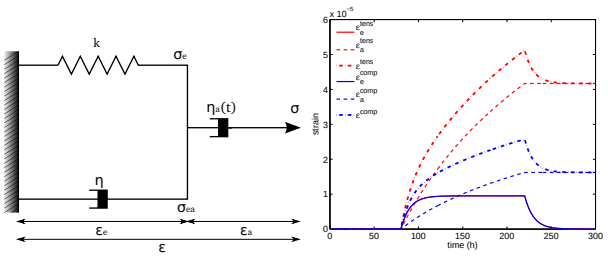

(a) 1D model

(b) $\epsilon_{kv}, \epsilon_{am}$ and ϵ_{tot} in tension and in compression

Figure 3: The proposed model for concrete creep

The system 4 can be extented to a three dimensionnal problem thanks to the relationships 6 where ν_c is creep Poisson's coefficient.

$$\dot{\boldsymbol{\epsilon}}_{bc} = \dot{\boldsymbol{\epsilon}}_{kv} + \dot{\boldsymbol{\epsilon}}_{am} \tag{6a}$$

$$\dot{\boldsymbol{\epsilon}}_{kv} = \frac{1+\nu_c}{k_{bc}}\dot{\boldsymbol{\sigma}}_e - \frac{\nu_c}{k_{bc}} tr\dot{\boldsymbol{\sigma}}_e \mathbb{1} \tag{6b}$$

$$\dot{\boldsymbol{\epsilon}}_{kv} = \frac{1+\nu_c}{\eta}\boldsymbol{\sigma}_{ea} - \frac{\nu_c}{\eta} tr\boldsymbol{\sigma}_{ea} \mathbb{1} \tag{6c}$$

$$\dot{\boldsymbol{\epsilon}}_{am} = \frac{1+\nu_c}{k_{bc}\tau}\langle\boldsymbol{\sigma}_\alpha\rangle - \frac{\nu_c}{k_{bc}\tau} tr\langle\boldsymbol{\sigma}_\alpha\rangle \mathbb{1} \tag{6d}$$

$$\boldsymbol{\sigma}_\alpha = \boldsymbol{P}\boldsymbol{D}_\alpha\boldsymbol{P}^{-1} \tag{6e}$$

$$\boldsymbol{D}_\alpha = \langle\boldsymbol{D}\rangle_- + \alpha\langle\boldsymbol{D}\rangle_+ \tag{6f}$$

Evolution of the parameters The parameter k_{bc} of the Kelvin-Voigt chain is linked to degree of hydration ξ according to the relationships proposed by [9]:

$$k_{bc}(\xi) = k_\infty \frac{0.473}{2.081 - 1.608\overline{\xi}} \overline{\xi}^{0.62} \tag{7}$$

in which k_∞ is the final stiffness of the spring, and $\overline{\xi}$ is defined by the equation 8.

$$\overline{\xi} = [< \frac{\xi(t) - \xi_0}{\xi_\infty - \xi 0} >_+]^{0.6} \tag{8}$$

where ξ_0 is equal to 0.1, it is the mechanical percolation threshold, over this degree of hydration concrete begins to perform like a solid. ξ_∞ is the final hydration degree.

Identification of basic creep parameters The modeling is validated against a work done by M.Briffaut [6], creep tests at early age have been conducted in compression and in tension at different age of loading. Strain evolutions predicted by the parameters in the table 2.2 are plotted on the figure 4.

Table 2: Basic creep parameters

$k_\infty(GPa)$	160
$\tau(h)$	3
$\eta_a(GPa)$	42
α	1.69

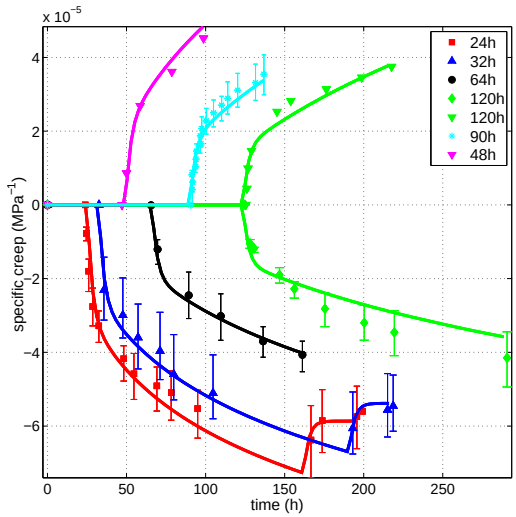

Figure 4: Comparison between simulated (thick lines) and experimental evolutions of strains from [6]

2.3 Modeling of autogenous shrinkage

The autogenous shrinkage ϵ_{au} is a consequence of the Le Chatelier contraction, so it is strongly linked to the degree of hydration. The measurement of its amplitude does not meet a general consensus. Indeed, depending on the used method very different results can be obtained for a same concrete [5]. The modeling is compared to the experimental results (Fig. 5) obtained thanks the device BTJADE [4]. An expansion is measured at the beginning of the hydration.

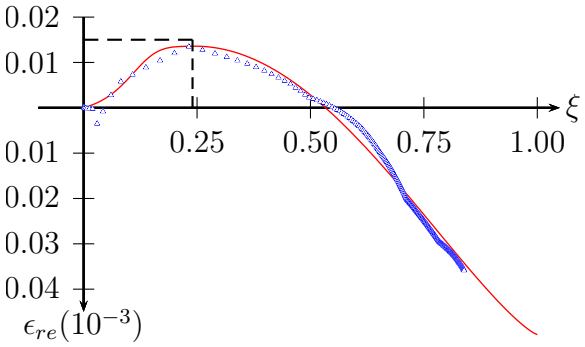

Figure 5: Evolution of ϵ_{au} versus the hydration degree

2.4 Elastic-damage behavior

Elastic model The elastic Poisson ratio ν and the Young modulus E are related to the degree of hydration thanks to the relationships (Eq. 2.4) proposed in [10] where ν_∞ is the final Poisson ratio, ν_0 is the Poisson ratio when concrete is still liquid, E_∞ is the final Young modulus and β is a constant. The elastic parameters are given in the table 2.4. The creep Poisson ratio ν_c is assumed equal to the elastic one.

$$\nu(\xi) = \nu_0 e^{-10\frac{\xi}{\xi_\infty}} + (\nu_\infty - \nu_0 e^{-10}) sin\left(\frac{\pi}{2}\frac{\xi}{\xi_\infty}\right) \tag{9a}$$

$$E(\xi) = E_\infty \langle \frac{\xi - \xi_0}{\xi_\infty - \xi_0} \rangle_+^\beta \tag{9b}$$

Table 3: Elastic parameters

ν_∞	0.2
ν_0	0.5
$E_\infty(GPa)$	32
β	0.62

Elastic-damage model A classical elastic damage modeling is used, the decrease of the stiffness in tension is governed by the equation 10 in which the damage variable D ,the effective stress tensor $\tilde{\boldsymbol{\sigma}}$ and the total strain tensor $\boldsymbol{\epsilon}$ are introduced.

$$\boldsymbol{\sigma} = (1 - D)\tilde{\boldsymbol{\sigma}} \tag{10a}$$

$$\dot{\tilde{\boldsymbol{\sigma}}} = E(\xi)(\dot{\boldsymbol{\epsilon}} - \dot{\boldsymbol{\epsilon}}_{bc} - \dot{\boldsymbol{\epsilon}}_{au} - \dot{\boldsymbol{\epsilon}}_{th}) = E(\xi)\dot{\boldsymbol{\epsilon}}_{el} \tag{10b}$$

The evolution of the damage variable is calculated according to following relationships where the Mazars' strain $\tilde{\epsilon}$ is introduced [13] [2] and κ_0 is the tensile strain threshold:

$$\tilde{\epsilon} = \sqrt{\langle \boldsymbol{\epsilon}_{el} \rangle_+ : \langle \boldsymbol{\epsilon}_{el} \rangle_+} \tag{11}$$

$$\begin{aligned} &\text{if } \tilde{\epsilon} > \kappa_0 \text{ then } : \\ &\quad D = 1 - \frac{\kappa_0}{\tilde{\epsilon}}\left((1 + A_t)exp(-B_t\tilde{\epsilon}) - A_t exp(-2B_t\tilde{\epsilon})\right) \\ &\text{if } \tilde{\epsilon} \leq \kappa_0 \text{ then } : \\ &\quad \dot{D} = 0 \end{aligned} \tag{12}$$

The tensile strain threshold is a function of the hydration degree ξ according to the equation 13

in which f_∞^t is final tensile strength of the concrete.

$$\kappa_0(\xi) = \frac{f_t(\xi)}{E(\xi)} = \frac{f_t^\infty \overline{\xi}^\gamma}{E(\xi)} \tag{13}$$

In order to avoid mesh dependency, a characteristic length l_c is introduced and correlated to the fracture energy G_{ft} and to the dissipated energy density g_{ft} at failure in tension (Eq. 14).

$$g_{ft} = \frac{G_{ft}}{l_c} \tag{14}$$

The fracture energy is function of ξ (Eq. 15) and the dissipated energy is calculated according to the equation 16.

$$G_{ft}(\xi) = G_{ft}^\infty \overline{\xi}^\gamma \tag{15}$$

$$g_{ft}(\xi) = f_t(\xi)\left(\frac{(1 + A_t/2)}{B_t}\right) \tag{16}$$

The damage parameters are given in the table 2.4.The lack of experimental data leads to take usual values for these parameters.

Table 4: Damage parameters

$f_t^\infty(MPa)$	2.5
$G_{ft}(J.m^{-2})$	48
A_t	1
γ	0.46

3 INFLUENCE OF THE CREEP DISSYMETRY ON THE STRESS STATE

A review of literature shows that there is not any consensus on the basic creep dissymetry (Fig.1). Even if the different works have been done under very different testing conditions (age of loading, curing, mix of concrete, samples' geometry), the influence of this dissymetry will be discussed based on the study of a massive wall poured on a raft foundation.
The data from M. Briffaut [5] are taken as a reference, in first approach, the ratio of the compressive basic creep divided by the tensile basic creep can be three times higher [15] or three times lower [11] than this reference. To take into account these fluctuations, the coefficient α is multiplied accordingly.
Because of the symmetry of the problem, only one half of the studied structure is presented on the figure 6 and plane strain conditions are assumed, since the lenght of the wall is equal to 30 m. For the thermal problem, a Newton's law for the heat exchange is assumed on the red faces ($h = 10\ W.m^{-2}.K^{-1}$) and the temperature $T = 7°C$ is imposed on the blue faces. The initial temperatures T_{wall}^i and $T_{foundation}^i$ are presented on the figure 6. The mechanical behavior of the foundation is assumed elastic with a Young modulus $E = E_\infty$.

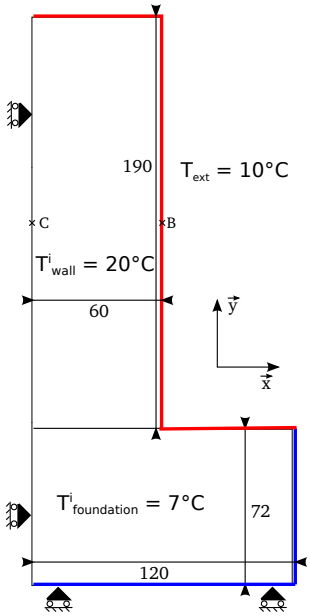

Figure 6: Geometry of the wall

3.1 Elastic simulation with creep

In this part, the structure remains elastic, there is not any damage. The influence of the parameter α is studied, the choice of the parameters is based on the work done by M. Briffaut (Tab. 2.2). The analysis is done for the elastic case without creep and for three different values of α: $\alpha = \frac{1.69}{3}$, $\alpha = 1.69$, $\alpha = 1.69 \times 3$. The evolution of the stresses σ_{zz} and σ_{yy} at the centre (point C) and at the surface (point B) of the structure are plotted on the figure 7 and 8 .

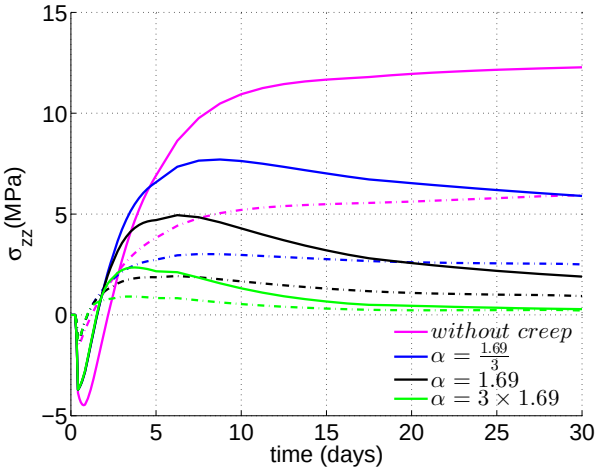

Figure 7: Evolution of the stresses σ_{zz} versus time at the centre (thick lines) and at the surface (dashed lines)

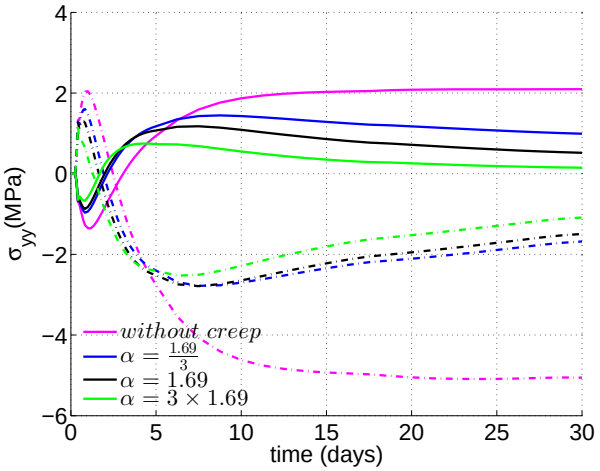

Figure 8: Evolution of the stresses σ_{yy} versus time at the centre (thick lines) and at the surface (dashed lines)

As expected, creep relaxation has to be considered to not overestimate the residual stresses at the end of the early age. On the figure 7, the influence of the coefficient α is underlined, high values for α leads to a decrease of the stresses in the concrete when it is under tension. The evolution of the stress σ_{yy} on the figure 8 is a consequence of the temperature gradient along the horizontal axis $\overrightarrow{grad}_x T$, the impact of α is less highlighted. Contrary to the evolution of σ_{zz}, the value of α bears on the compressive and the tensile state: the restraint is total along the $\overrightarrow{z}$ axis when the partial restraint caused by the gradient of temperature $\overrightarrow{grad}_x T$ is reduced by creep.

3.2 Elastic-damage simulation with creep

Now, the damage variable is introduced, the influence of the parameter α on this variable is studied. The figure 3.2 shows the damage field for three values of α at the end of the early age (one month after the casting of the concrete). Several significant cracks have been reported after the construction of the wall in the central and the interfacial areas. However, the plane strain condition overestimate the restraint along the $\overrightarrow{z}$ direction and as well the damage is . As previously mentioned, the impact of the value of α is significant, the final damage field is hugely dependent on it. For $\alpha = \frac{1.69}{3}$, the structure is severely damaged when for $\alpha = 1.69 \times 3$, the structure remains sound.

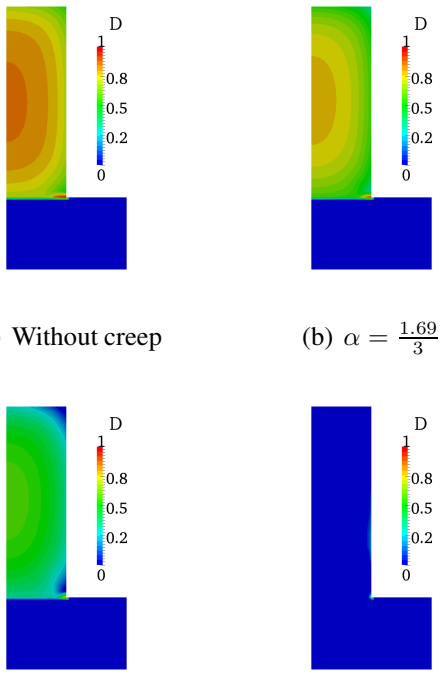

(a) Without creep (b) $\alpha = \frac{1.69}{3}$

(c) $\alpha = 1.69$ (d) $\alpha = 3 \times 1.69$

Figure 9: Damage field at the end of the early age for different values of α

4 CONCLUSION

Most of the published works shows that there is not any consensus about the influence of the loading on the creep 's compliance. To take

account this possible dissymetry, a one dimensional modeling is proposed thanks to the parameter α, a creep Poisson's coefficient is introduced to analyze massive structures. The chosen modeling is characterized by its simplicity and its ability to introduce a difference between compression and tension. Comparisons with experimental data are satisfying.
A massive structure is studied at the early-age, several values of α are used to convey the uncertainty about this parameter. The results show that the creep's consequences on the behavior of the wall are strongly dependent on it. Indeed, the final damage field is severely damaged if the compressive creep is higher than the tensile creep but it remains close to zero for an inverse dissymetry.
A numerical analysis of a typical massive structure at early age make evident the importance of a better understanding of creep characteristics. More experimental tests are needed to fill this gap of knowledge.

REFERENCES

[1] ATRUSHI, D. S. *Tensile and Compressive Creep of Early Age Concrete: Testing and Modelling*. PhD thesis, The Norwegian University of Science and Technology, Trondheim, Norway, Mar. 2003.

[2] BENBOUDJEMA, F., AND TORRENTI, J. Early-age behaviour of concrete nuclear containments. *Nuclear Engineering and Design 238*, 10 (2008), 2495–2506.

[3] BISSONNETTE, B., AND PIGEON, M. Tensile creep at early ages of ordinary, silica fume and fiber reinforced concretes. *Cement and Concrete Research 25*, 5 (1995), 1075–1085.

[4] BOULAY, C. Développement d'un dispositif de mesure du retrait endogène d'un béton au jeune âge. In *Huitième édition des Journées Scientifiques du Regroupement Francophone pour la Recherche et la Formation sur le béton (RF)2B* (Jan. 2007).

[5] BRIFFAUT, M. *Étude de la fissuration au jeune âge des structures massives en béton: influence de la vitesse de refroidissement, des reprises de bétonnage et des armatures*. PhD thesis, ENS de Cachan, 61, avenue du Président Wilson, 94235 CACHAN CEDEX (France), Oct. 2010.

[6] BRIFFAUT, M., BENBOUDJEMA, F., TORRENTI, J., AND NAHAS, G. Early age basic creep for massive structures : experimental results and rheological modelling. *Construction and Building Materials Journal* (2011).

[7] BROOKS, J. J., AND NEVILLE, A. M. A comparison of creep, elasticity and strength of concrete in tension and in compression. *Magazine of Concrete Research 29*, 100 (1977), 131 –141.

[8] DARQUENNES, A. *Comportement au jeune âge de bétons formulés à base de ciment au laitier de haut-fourneau en condition de déformations libre et restreinte.* PhD thesis, Université libre de Bruxelles, Nov. 2009.

[9] DE SCHUTTER, G. Degree of hydration based Kelvin model for the basic creep of early age concrete. *Materials and Structures 32*, 4 (1999), 260–265. 10.1007/BF02479595.

[10] DE SCHUTTER, G., AND TAERWE, L. Degree of hydration-based description of mechanical properties of early age concrete. *Materials and Structures 29* (1996), 335–344. 10.1007/BF02486341.

[11] LI, H., WEE, T., AND WONG, S. Early-Age Creep and Shrinkage of Blended Cement Concrete. *Materials Journal 99*, 1 (Jan. 2002), 3–10.

[12] MASSE, M. B. Étude du comportement déformationnel des bétons de réparation. Master's thesis, École polytechnique de Montréal, Aug. 2010.

[13] MAZARS, J. A description of micro- and macroscale damage of concrete structures. *Engineering Fracture Mechanics 25*, 5–6 (1986), 729–737.

[14] REVIRON, N. *Etude du fluage des bétons en traction. Application aux enceintes de confinement des centrales nucléaires à eau sous pression*. PhD thesis, ENS de Cachan, Mar. 2009.

[15] ROSSI, P., TAILHAN, J.-L., MAOU, F. L., GAILLET, L., AND MARTIN, E. Basic creep behavior of concretes investigation of the physical mechanisms by using acoustic emission. *Cement and Concrete Research 42*, 1 (2012), 61–73.

[16] ULM, F.-J., AND COUSSY, O. Couplings in early-age concrete: From material modeling to structural design. *International Journal of Solids and Structures 35*, 31–32 (1998), 4295–4311.